Evolution of the “last” invariant curve in a family of area preserving maps

Carles Simó[(1)] and Dmitry V. Treschev [(2)]

[(1)] Departament de Matemàtica Aplicada i Anàlisi, Universitat de Barcelona, Gran Via 585, 08007 Barcelona, Spain.
[(2)] Department of Mathematics, Moscow State University, Moscow, Russia.

Abstract

Area preserving maps appear in a natural way in Poincaré sections of Hamiltonian systems with two degrees of freedom. Around an elliptic fixed point there are, generically, invariant curves bounding a stable region. This note proposes a numerical method, strongly based on the dynamics, to locate the “last” invariant curve, that is, the boundary of the stable connected component containing the elliptic fixed point. The variation of this curve and the corresponding rotation number when a parameter is changed are displayed. Several examples illustrate the procedure and some properties are discussed.

1 Introduction: The problem

One of the fundamental problems in Hamiltonian dynamics, in the simplest non trivial case, that is, with two degrees of freedom, is the existence of stable regions of the phase space. If the system has a periodic orbit, γ, it is possible to use a Poincaré section transversal to it, Σ, to reduce the study of the Hamiltonian, H, on a fixed level of the energy, h, to the analysis of an area preserving map, the related Poincaré map, $F:\Sigma\rightarrow\Sigma$, around a fixed point, p_0. If this one is elliptic, that is, $\mathrm{spec}(DF(p_0))\in\mathbb{S}^1\setminus\{\pm 1\}$ or, equivalently, $|\mathrm{trace}(DF(p_0))|<2$, then, under a generic *twist condition* the KAM theorem assures the existence of invariant curves around p_0. These curves bound the motion near the fixed point and, so, there is an invariant disk under F and, therefore, a stable solid torus on $H^{-1}(h)$. In fact the twist condition everywhere is not essential, because in the non–twist case the existence of invariant curves is also obtained under natural generic conditions (see [12] for a theoretical study, [13] for the occurrence in n–body problems and [2] for a detailed analysis of the tripling bifurcation and several additional examples).

The problem that we address in this note is the determination of the maximal stability disk around p_0. Indeed, the KAM theorem is of local nature, and despite it is certainly true that it is possible, with the help of rigorous symbolic manipulation with control of the remainder, to produce high order normal forms around p_0, allowing to improve the range of validity of the theorem, it seems to us that this is far from efficient. A different approach would be the development of normal forms around the invariant curve for intermediate values of the perturbation parameter, but this seems not to be carried out till present.

To obtain the maximal disk is equivalent to produce the “last” invariant curve around p_0. Note that other stable domains can exist *outside* the disk and “related” in some way to the fixed point. We refer, of course, to chains of island beyond the last invariant curve, but emanating, when moving some parameter, from the fixed point.

It is natural also to consider a system not as isolated but inside some parametric family. As a key parameter, in the present case, is the rotation (or the trace of the differential) at the fixed point, it is enough to consider one–parameter families allowing the trace to move in the full admissible range $(-2, 2)$. Hence we want to see also how the last invariant curve evolves as a function of a parameter. As representative magnitudes of this evolution we can consider the *area* enclosed by the last invariant curve and the *rotation number* of the same curve.

All these considerations can be applied when we study periodic points of the map F. If $F^n(p_0) = p_0$ for some $n \in \mathbb{N}$, $n > 1$ and $F^j(p_0) \neq p_0$ for $j = 1, \ldots, n-1$ simply replace F by F^n in what follows. In fact the seminal example of this study was motivated by our interest in the stability areas around periodic points in the previous work [14]. There, beyond general results, the case of points of period 3 of the *separatrix map* is analyzed. We shall use this map in the examples below, but "any" non degenerate family of maps could do. Non degenerate means here that the trace covers monotonically the range $(-2, 2)$ when the parameter moves.

2 An algorithm

The algorithm we propose to detect the last invariant curve consists of several steps. All of them are strongly guided by the dynamics of the area preserving map. To begin with we assume that the fixed point is p_0 and we consider a ray going away from p_0 and parameterized by the distance, s, to p_0 (an arc going away from the fixed point, parameterized by the arc length for instance, could also be used). The point of parameter s will be denoted as $q(s)$. We assume *explicitly* that the invariant curves around p_0 are transversal to this ray. According to Birkhoff theorem, this always holds if the map is twist in the domain we are interested in. However, the transversality we mentioned is weaker than the twist condition. Below we will see that the twist condition is violated in our example (see figures 5 and 6 and the corresponding discussion). We also assume that there is really a last curve, in the sense that points far enough from p_0 escape, and that this curve (or an approximation to the last one) is smooth enough, at least within the computer resolution. Then

1. Fix a maximal number of iterations, N. A value between 10^4 and 10^5 can be suitable, but if the map is obtained by integration of a flow, perhaps it is convenient to start with smaller values. Fix also a maximal distance, $R_{\max}$, to q_0 such that if $\text{dist}(F^j(q), q_0) > R_{\max}$ for some $j \leq N$, we can consider that the point q *escapes* and otherwise that it *remains*. Fix also some tolerance, δ_s, for the determination of s. Let $s_1 = 0$ and $s_2 = s_{\text{large}}$ such that $q(s_1) = p_0$ remains bounded under iteration while $q(s_2)$ escapes. Use bisection to obtain a value $s = s_b$ such that $q(s_b)$ remains and $q(s_b + \delta)$, $\delta < \delta_s$, escapes. Certainly the intersection of the last invariant curve with the ray can not have a parameter s larger than $s_b + \delta_s$. This ends the first step, with $s = s_b$. See later the description of the results for alternative approaches to this first step.

   Now we can consider why $q(s_b)$ has not escaped. There are several reasons for that, and the remaining steps will try to refine this preliminary determination (very rough in many cases):

- It belongs to an invariant curve, as desired. This one can be considered as an approximation to the last invariant curve and the process can be stopped.
- It belongs to an island outside the last invariant curve around q_0. It is not admissible.
- It belongs to a chaotic zone for which most of the points will escape, but the rate of diffusion is too slow to escape in N iterates. It has to be discarded, too.

2. Let $\mathcal{P} = \{F^j(q(s)),\ j = 0, 1, \dots, N\}$ be the computed segment of the orbit of a point $q(s)$ which remains. We shall start now with $s = s_b$. First we proceed to "sort" the points in $\mathcal{P}$, which are assumed to be in a smooth enough curve, "along" this curve. To this end choose a normalized vector, v_0, transversal to the ray through $q_0 := q(s)$. Let $\mathcal{H}_0$ be the half plane defined by $\{z \in \mathbb{R}^2 \mid (v_0, z - q_0) > 0\}$, where $(\ ,\ )$ denotes the scalar product. We look in $\mathcal{H}_0$ for the closest point to q_0 in $\mathcal{P}$. To this end it is suitable to sort first the points in $\mathcal{P}$ by the value of some of the coordinates or of the projection, $\pi(z)$, on some 1D subspace. This part of the process has a cost $O(N \ln N)$ but it saves costs of the order $O(N^2)$ in the subsequent steps. Then it is only required to look to points $z \in \mathcal{P}$ such that $\pi(z)$ is close to $\pi(q_0)$ and a small set of points (O(1)) has to be examined. Denote as q_1 the point determined in this way. Then define a new normalized vector, v_1, by $v_1 = (q_1 - q_0)/||q_1 - q_0||$.

   With this vector v_1 define the corresponding half plane $\mathcal{H}_1$ and proceed as before to determine the closest point, q_2, to q_1 in $\mathcal{H}_1$. Iterate the process until all the points are "sorted" along the tentative curve. As soon as a point has been "put on his place on the curve" it should be marked as non able to be selected again. This do not applies to the initial point q_0, because if $\mathcal{P}$ is really a closed curve we should return to it at the end. If at some step we are not able to find the corresponding $q_{m+1} \in \mathcal{H}_m$ we conclude that $\mathcal{P}$ is not a curve. The same thing happens if we return to q_0 before exhausting $\mathcal{P}$. This can happen, for instance, if $q(s)$ belongs to an invariant curve inside some island but outside the last invariant curve we seek.

3. During the previous process attention has to be paid to two additional facts:

   - The distance from a point q_m to the next one q_{m+1}. It should not be too large. Otherwise, perhaps we are crossing a gap in a cantorus. To this end we must estimate an "average" distance between the points. This can be done by taking the perimeter of the smallest (square, for instance) box which contains $\mathcal{P}$ and dividing by the number of points. One should allow for a "generous" factor to account for the possible folds of the curve and for the lack of good equidistribution along it, if the rotation number has a continued fraction expansion whose initial quotients are relatively large. This bound on the distance can already be used in the previous sorting of the values of $\pi(\mathcal{P})$. In particular this can discard cases in which $q(s)$ belongs to some island.
   - The angle between two consecutive vectors v_m and v_{m+1}. It should be not too large, too. It will be large at some place or another if $\mathcal{P}$ is in fact a narrow (or, a fortiori, thick) cloud of points belonging to a chaotic zone, and this will allow to discard this possibility.

     However this posses a difficulty. If the last invariant curve leaves outside (or inside) some nearby saddles, it can happen that it approaches the stable and unstable manifolds of this saddle. The curve “bends” strongly in the vicinity of the saddle. This could lead to discard a correct estimate of the last invariant curve. There are two considerations to be made. The first one is that if an invariant curve comes close to a saddle the dynamics (of some power of the map equal to the period of the saddle) is quite slow. Then we have an accumulation of points of $\mathcal{P}$ in this region and the angle between consecutive points along the curve can be moderated by this accumulation. The second consists, simply, in increasing the value of N. This is a typical situation for “last” invariant curves. Usually, they have a hyperbolic periodic orbit, of a relatively low order, nearby.

4. Finally, if all the points in $\mathcal{P}$ have been exhausted, the last point, q_N, coincides with q_0 and the distance and angle tests are passed along the full curve, we still have another test which consists in the determination of the rotation number. Up to now we have used the geometry of the invariant curve and our general knowledge of the dynamics, but not the dynamics on the curve itself. Every point in $\mathcal{P}$ is an iterate of $q_0 : q_{k(m)} = F^m(q_0)$, and $k(m)$ must depend on m as happens on a rigid rotation of $\mathbb{S}^1$ with an unknown rotation number ρ. If we do not know a priori the “sense” of traveling it is possible that we obtain $1-\rho$ instead of ρ (this depends on the initial choice of v_0). But this is not a problem.

   First we have to compute the *index inside the curve* of each iterate, that is, the function $k(m)$. Then we can count the *number of revolutions* of the successive iterates. This is done as follows: If $k(m+1) > k(m)$ the number of revolutions, $\text{rev}(m+1)$ is equal to $\text{rev}(m)$. Otherwise $\text{rev}(m+1) = \text{rev}(m)+1$. Then we look at all the successive couples of consecutive points along the tentative curve. Let q_j and q_{j+1} one of these couples. Each one has an associated number of iterates, ($k^{-1}(j)$ and $k^{-1}(j+1)$,) and the corresponding number of revolutions, ($\text{rev}(k^{-1}(j))$ and $\text{rev}(k^{-1}(j+1))$).

   Let μ be the quotient between the difference of the number of revolutions and the difference of the number of iterates. If $\mu > 1/2$ replace μ by $1-\mu$. Before starting to look at the points let $\rho_{\text{inf}} = 0$ and $\rho_{\text{sup}} = 1/2$. At the end of the process ρ_{inf} and ρ_{sup} will contain lower and upper estimates of ρ. If $k^{-1}(j+1) > k^{-1}(j)$ then we replace ρ_{inf} by the maximum between μ and ρ_{inf}. If $k^{-1}(j+1) < k^{-1}(j)$ then we replace ρ_{sup} by the minimum between μ and ρ_{sup}. If during the process it happens $\rho_{\text{inf}} \geq \rho_{\text{sup}}$, we have something not compatible with the assumed dynamics of the curve, and it is discarded. Otherwise we have estimates of the rotation number which should agree up to $O(N^{-2})$.

   Note that there are other methods to compute the rotation number of a tentative invariant curve of an area preserving map, but we have preferred this more topological approach (also because the points have been already sorted). They are based on the Fourier analysis of a time series consisting of any of the coordinates of the successive iterates $F^j(q_0),\ j = 0, \ldots, N-1$. These methods have, as general purpose to produce a refined estimate of frequencies (see [6], [7] and [4]). They have a similar global cost ($O(N \ln N)$ for every checked value of s) and are able to produce better estimates provided the data are smooth enough. In the case of curves passing very close to saddles the Fourier series decay slowly and the results can be not very precise. Of course, in this case also the method proposed here can produce poor estimates. A very small change in the final s adopted will almost not affect the area bounded by the last invariant curve, but certainly affects the value of ρ. Indeed, if $\rho = p/q + \varepsilon,\ p/q \in \mathbb{Q}$, then F^q produces points in the orbit moving slowly near the saddle. If d is the minimum distance of the orbit to the saddle and λ the dominant eigenvalue under F^q, then $|\varepsilon| = O(q^{-2}\lambda^{-1}|\ln(d)|$.

5. If for one reason or another the set taken as tentative last invariant curve is discarded, then we must restart the full process (except the first step) by replacing s by some smaller amount. The choice $s - \delta_s$ is the reasonable one. It is also possible to skip the test based on the estimates of the rotation number and use it later as an additional check.

6. At the end, the area enclosed by the last invariant curve is easily estimated from the final set $\mathcal{P}$. Indeed, we end up with a polygonal approximation to an invariant curve, the polygon being determined by all the sides of the form $\overline{q_m q_{m+1}}$. If the coordinates used are (x, y), one has to compute $\int y\,dx$. It can be approximated by $\sum_{m=0}^{N-1} \frac{1}{2}(y_{m+1} + y_m)(x_{m+1} - x_m) = \sum_{m=0}^{N-1} \frac{1}{2}(y_m x_{m+1} - y_{m+1} x_m)$.

This finishes the description of the proposed algorithm.

3 Some results

All the illustrations presented here have been produced with the so called *separatrix map*, but several other maps, even coming from sections of Poincaré of two degrees of freedom Hamiltonians (e.g., the Hénon–Heiles problem) have been tested with similar results. The version of the separatrix map we use here is a scaled version of the one presented in [3] and [16]. As said before, this map was taken to display an example in [14] about the existence of not too small islands, inside the loops formed by the stable and unstable manifolds of a saddle. Furthermore the set of parameters for which very simple islands (we restricted, for simplicity, to period 3) exist is quite abundant, with a limit density when the perturbation parameter goes to zero (see [14] for the details).

The separatrix map is defined on the cylinder $\mathbb{S} \times \mathbb{R}$, where $\mathbb{S} = \mathbb{R}/\mathbb{Z}$, by $\mathrm{SPM} : (x, y) \to (x', y')$, with $y' = y + \sin(2\pi x),\ \ x' = x + c + d\ln(|y'|) \pmod 1$. It depends on two parameters, c mod 1 and d, but typically we shall consider d as fixed and c as the only true parameter. The value of d has been selected carefully so that the areas of the islands inside the loops made by the two separatrices ($y = 0$, unstable manifold, and $y = -\sin(2\pi x)$, stable manifold) are relatively large. The adopted value is $d = 0.061388313$ (or, more precisely, $d = (\ln 11872620)^{-1}$), and we keep it on all the figures displayed here.

We look at the periodic orbit of period 3 which has some (exactly 2) of the points inside the loops. This orbit has a point on $x = 0$, a property which simplifies the analysis and the computations. Due to the symmetries of the separatrix map, there is also a companion orbit with a similar behavior. We are interested in values of c such that this orbit is elliptic and has a related domain (island) of stability as large as possible. Other big islands can appear (see Fig. 4, where we also display the separatrices), but all the iterates are outside the loops. Note that the separatrix map has a singularity when a point is on the stable manifold.

Figure 1 shows the relative area (this means the area divided by the area of the loop) of each one of the period 3 islands having iterates inside the loops, as a function of the trace at the periodic point. It has been found that for $c = 0.383747662$ the trace is equal

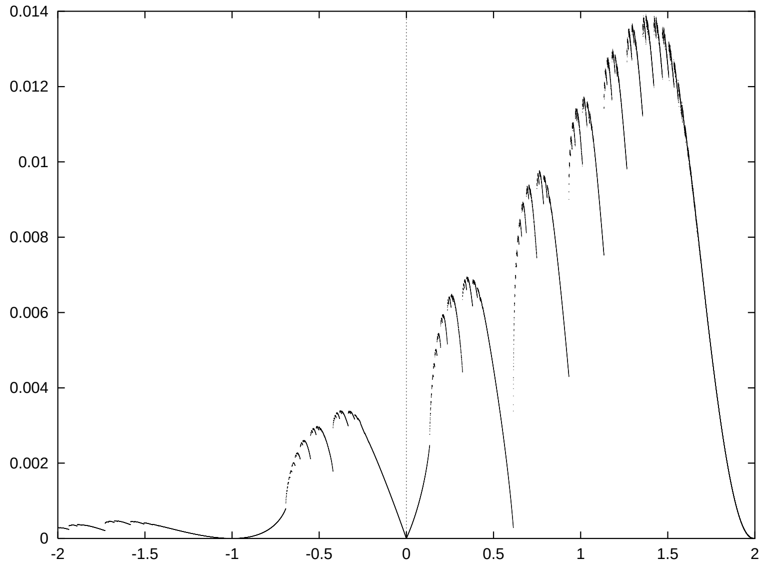

Figure 1: Fraction of the area of the loop inside the island for $d = 0.061388313$, as a function of the trace at the elliptic point.

to $+2$, and it equals -2 for $c = 0.4110407593$. This is not the only range of c producing elliptic periodic points inside the loops, but it is certainly the one associated to the largest islands. A total of 38096 values of c have been used in this range.

When the trace tends to $+2$ the area of the island goes to zero. Other values appear for which the area goes to zero. They correspond to elliptic points having eigenvalues, λ, which are cubic (trace$= -1$) or quartic (trace$= 0$) roots of the unity. The instability in the case of the cubic root is generic. In the case of the quartic one it depends on the value of some coefficient in the normal form, so that both the stability and instability can occur in an open way, depending on the value of this coefficient. For instance, the Hénon conservative map, in contrast with the separatrix map, has a stable fixed point when trace$= 0$. See [2] or [12] when trace$= -1$ for the Hénon map. For a complete analysis of the stability of fixed or periodic points of parabolic type (that is, $|\text{trace}| = 2$) and, hence, by using a power of the map, of any case with eigenvalue equal to a root of the unity, we refer to [10].

The diagram has a clear fractal structure. Furthermore the plot looks very similar, except by scalings, for rotation numbers in $[1/5, 1/6]$, $[1/6, 1/7]$, $[1/7, 1/8]$, etc. The maximum is achieved for a rotation number in $[1/9, 1/10]$. With less detail a similar picture can be found in the case of the Hénon conservative map in [9]. But this picture includes also the area of the islands outside the last invariant curve, as non–escaping area. At this point it can be worth to point out that for the Hénon map a quick estimate of the location of the last invariant curve can be done as follows (it could be used as step 1 in the algorithm): The elliptic fixed point is born by an elliptic–hyperbolic bifurcation at the same time that an hyperbolic one. Computing the stable (or unstable) manifolds of that point gives a quite precise location of the last invariant curve. This method is not so suitable in the case of the separatrix map because of the singularity appearing for $y = 0$ and also because from $c = 0.4080828197$ on, the hyperbolic point (which was on $x = 0$ as the elliptic one) changes stability and becomes elliptic. A further description of the relation between destruction of invariant curves (or KAM tori) and the stable/unstable manifolds of lower dimensional invariant objects can be found in [13].

Figure 2 shows a magnification of Fig. 1, where the rotation numbers at the elliptic point and at the last invariant curve are shown. Note that in this subrange of c, for a fixed value of c the rotation number at the elliptic point is larger than on the last invariant curve. This is not always true, as we shall see later.

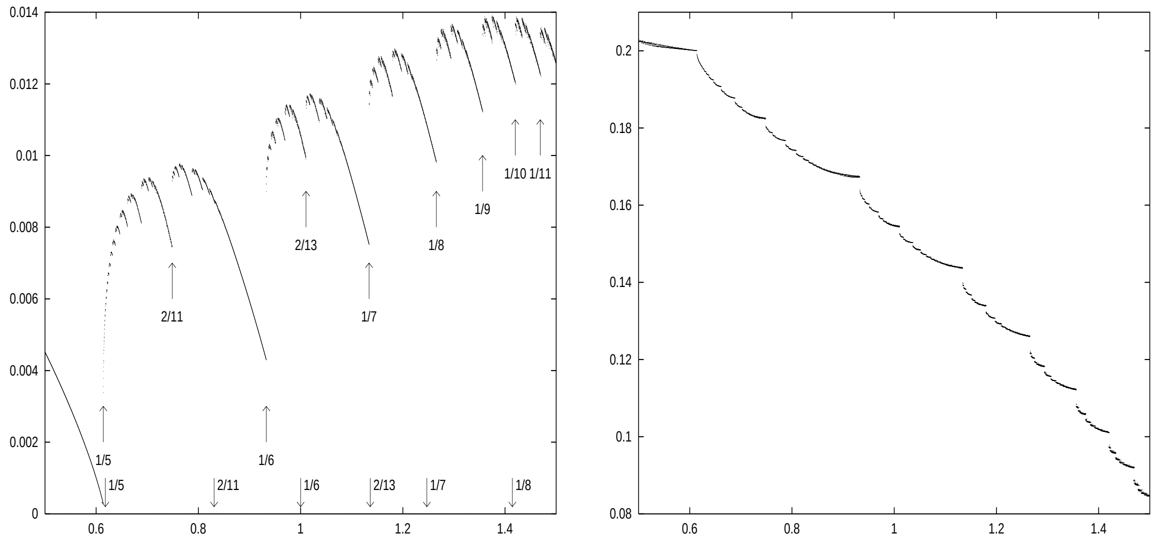

Figure 2: Left: Magnification of Fig. 1. Upwards arrows show the rational over which the rotation number on the last invariant curve jumps. Downwards ones the rotation number at the periodic point. Right: Rotation number on the last invariant curve as a function of the trace at the elliptic point.

On the right part of Fig. 2 it is clearly seen that the determination of the rotation number is more rough when the last invariant curve approaches a periodic saddle from inside. That is, on the points of this figure for which the graph is close to horizontal before jumping down. This agrees with the difficulty mentioned at the second point in steps 3 and 4 of the algorithm.

Figure 3 displays, for two nearby values of c, the different behavior of the last invariant curve. The rotation number of this last curve is close to $2/9$. The related satellite islands around the central elliptic point have period 9 and they give two revolutions before closing. This refers, of course, to the behavior which leaves the central point invariant, that is, not under SPM but under SPM^3. In the left plot these islands are outside the last invariant curve. In the right one they have moved inside. A similar behavior occurs when the rotation number of the last invariant curve "jumps over" any rational, "eating" or "expelling" a chain of satellite islands.

When a chain of resonant islands is either absorbed or expelled by the "last" invariant curve, both the area of the island and the rotation number of the last curve have a jump. It is interesting to compare these jumps. An heuristic argument relating the magnitudes of these jumps can be based on results of [15]. In [15] a symplectic perturbation of an integrable map of a cylinder into itself is considered near a resonance. Let the rate of the perturbation be of the order ε. Then it is well–known that the width of the resonance zone is of order $\sqrt{\varepsilon}$. In [15] it is proven that the difference of frequencies for the invariant curves bounding the zone is $O(\varepsilon)$ for analytic maps (for $\mathcal{C}^k$–smooth, $k < \infty$, the difference is also $O(\sqrt{\varepsilon})$). Assuming that the map we deal with in the vicinity of the last invariant curve can be regarded as not too far from integrable, one can expect that the jumps of the scaled area, $\Delta S/S$, and the jumps of the rotation number, $\Delta\rho$, we discuss above, should be related as follows: $|\Delta\rho|(|\Delta S|/S)^{-1/2} \simeq$ constant. Our numerical results do not

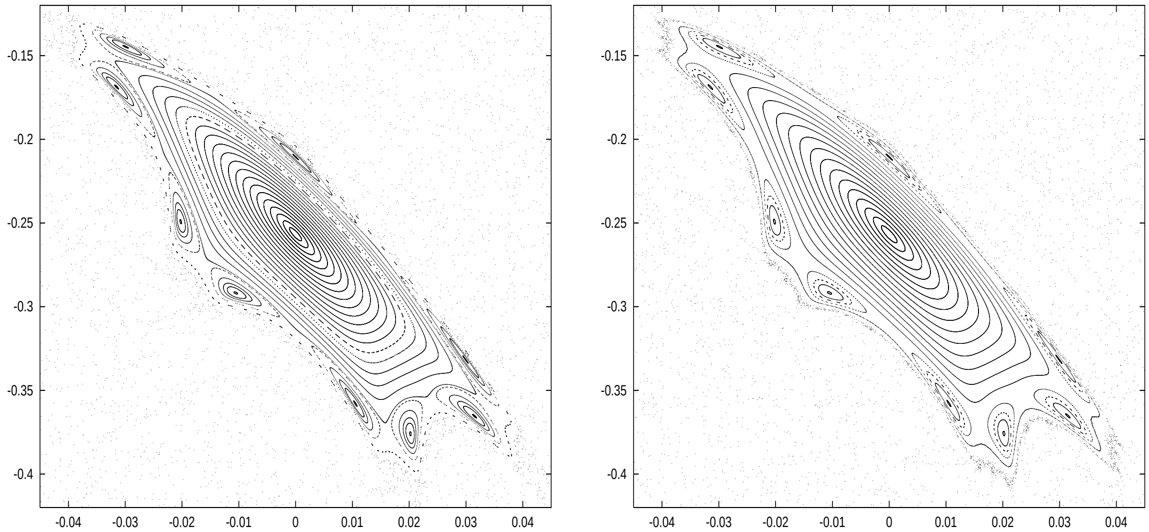

Figure 3: The invariant domain for $d = 0.061388313$ and $c = 0.39736637$ (left) or $c = 0.39736537$ (right). The rotation number of the last invariant curve is greater (resp. smaller) than 2/9 in the left (resp. right) case. Note that the position of the satellite islands is almost the same, but they are outside (resp. inside) the invariant curve in the left (resp. right) case.

obviously confirm this relation: for different resonances this quantity varies by a factor of the order of 1 to 4. To get this, one has to avoid neighborhoods of places where the area goes to zero: trace$= -1$ (order 3 resonance), trace$= 0$ (order 4 resonance), by the reasons presented above, then trace$= 2$ (close to the creation of the island) and a neighborhood of the jump over $\rho = 1/5$, by a different reason, to be presented below.

Two chains of 5 islands inside the last invariant curve appear in Fig. 4. Also two hyperbolic orbits of period 5 are clearly seen. This figure illustrates some nice shapes that the last invariant curve can have. On the right part of the figure we display the chaotic orbit of a single point. The "footprints" of the 2 chains of 3 periodic islands which have 2 islands each inside the loops are clearly seen. Two additional chains are completely outside the loops. Note that the chaotic orbit takes, essentially, all the area available between the "last" upper and lower invariant curves with the exception of the holes of the 12 islands.

We also want to remark that the big jump in the area inside the last curve when the rotation number of this one jumps over 1/5 is related to the existence of two of period–5 islands. By a very small increase of c with respect to the value used in Fig. 4 (this is equivalent to a small decrease on the trace at the central point, that is, we move to the left in Fig. 2), the 5 "fingers" of the figure become very thin, the curves containing the inner chain of islands, but not the outer one, are broken, and there appear period–5 invariant curves containing one island of each family and the intermediate saddle. Later on, the saddle and the inner island collapse and the "boundary of the fingers" is broken. The last invariant curve is very close to the central point and, outside, the outer period–5 islands remain. When this happens we are at the minimum of the area (trace $\simeq 0.61$ in Fig. 2). Other kinds of pathologies related to period 5 appear in [2].

Next we illustrate the lack of monotonicity of the rotation numbers when we consider the SPM as a family of maps depending on the parameter c. Figure 5 shows the following: Consider the position of the elliptic point we are discussing on $x_0 = 0$ and let y_{ell} be the value of the y coordinate. For a fixed value of c we can take values $y_0 > y_{\mathrm{ell}}$ as initial points

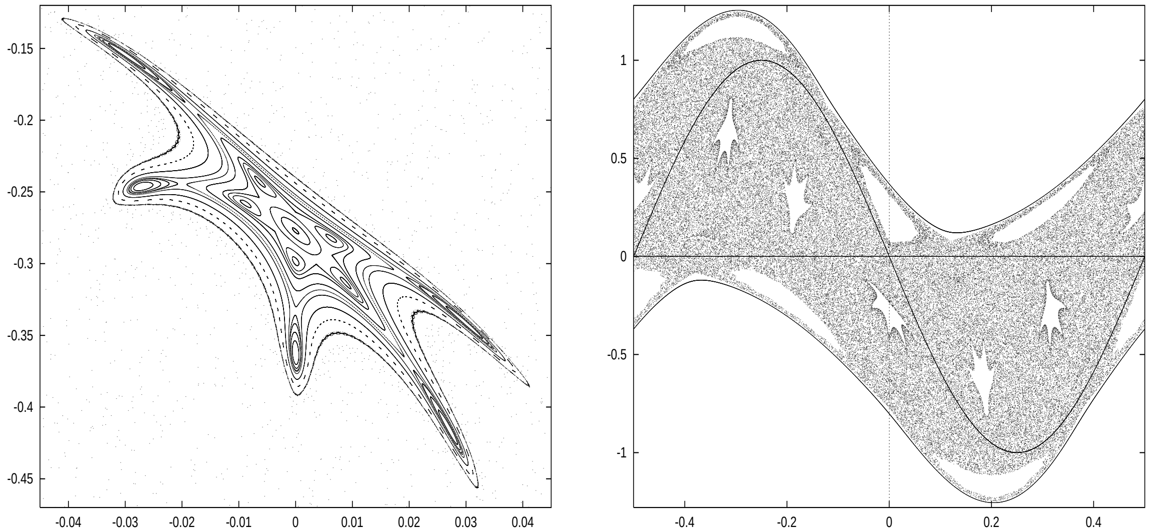

Figure 4: On the left an "artistic" stability domain with last invariant curve of rotation number slightly less than $1/5$. On the right a chaotic orbit for the same values of the parameters. The holes of four 3–periodic orbits are seen, the central one being the one corresponding to the left plot. Two of these orbits have all the iterates outside the loops of the separatrices. Same d as in the previous figures with $c = 0.395063131$. For completeness the separatrices are also displayed. Note that very close to this chaotic orbit (just 10^5 points are plotted, starting at $(0., -0.4)$) there are invariant smooth curves, which can be seen in the upper and lower part of the plot. These curves have initial points at $(0., 0.37)$ and $(0.5, -0.37)$. Note, however, that the value 0.37 could be replaced by 0.357838, still having an invariant curve, but so close to the chaotic zone that it would be hard to distinguish with the present scale.

up to the value, y_{last}, of y which gives the last invariant curve. Then the rotation number of the orbit of initial point (x_0, y_0) can be computed. If it is on an invariant curve we can use the topological method described in step 4 of the algorithm. Otherwise we can simply lift SPM to $\mathbb{R}^2$ and, after n iterates, producing $(x_0, y_0), (x_1, y_1), \ldots, (x_n, y_n)$, take x_n/n as an estimate of ρ. We keep the same name for the variables in the lift space. One can test several values of n to have reliable results. Inside a satellite island, in the inner part of the last invariant curve, the rotation number must be constant. The strongest difficulties to produce ρ appear in the chaotic zones confined by the last invariant curve, but apparently these zones are quite narrow and the numerical procedure had no difficulties.

Hence, for each selected value of c, a table of values of $\rho(y_0)$ for $y_{\text{ell}} < y_0 < y_{\text{last}}$ is available, and can be plotted on the (y, ρ) plane. This has been done in figure 5 for several values of c. The figure starts on the left part and continues on the right. The values of c giving a trace at the elliptic point which is close to -2 appear on the upper part at the left, while the ones having a trace close to $+2$ are located in the lower part at the right. For each one of the plotted curves the leftmost point corresponds to y_{ell} and the rightmost one to y_{last}. So this figure also gives an evidence of the size of the island (compare with figure 1). Indeed, for each one of the curves shown in figure 5, the difference between the right and left values of x gives an estimate of the "radius" of the last invariant curve. Figure 1 looks, roughly, as the square of this magnitude.

Going from top to bottom the rotation number at the elliptic point decreases (and, hence, the trace increases). The points corresponding to cubic and quartic roots of the unity are clearly seen on the left plot. At these two places there is a local variation of the monotonicity of the rotation number as a function of y. Before the cubic root of the unity,

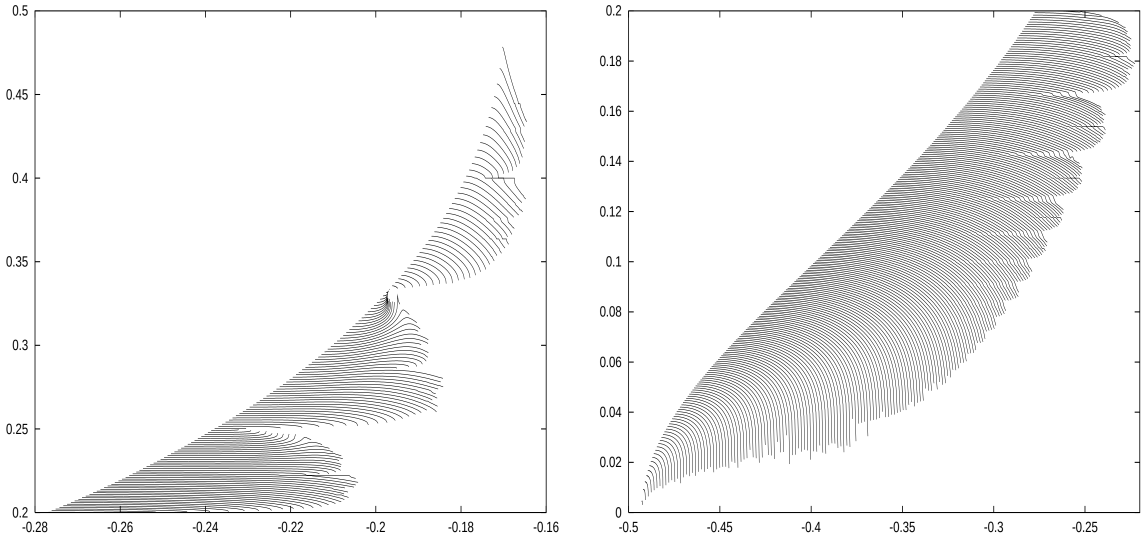

Figure 5: For the same value of d used in the previous figures, we display a plot of the rotation number on the invariant curves as a function of the value, y_0, of the y coordinate of the initial point on $x_0 = 0$. The left part covers from trace equal to -2 at the elliptic point up to the 1 to 5 resonance. The right part covers the remaining set of values. Each line corresponds to a fixed value of c. Note the lack of monotonicity in some domains.

the rotation number decreases as a function of y, while after that value it increases. The same thing occurs at trace $= 0$. For this map this is easily checked analytically by using normal forms. Between trace $= -1$ and trace $= 0$ we have that, locally near the elliptic point, there is a change in the monotonicity of ρ. This suggest that, when we look at the full plot of ρ for $y_{\text{ell}} < y_0 < y_{\text{last}}$, there is a good chance to find extrema of ρ, leading to a loss of the monotonicity. This is illustrated in more detail in figure 6. A range of values of the parameter for which the map do not satisfies the twist condition appears also for the Hénon map. We refer to [12] for a general presentation and several generic and non generic cases, and to [2] for a complete study of the Hénon map. Illustrations can be found in both papers. Furthermore, [13] presents the occurrence of the same phenomenon around the Hill's direct periodic orbit in the classical Hill's problem in Celestial Mechanics (and, hence, in the Restricted Three Body Problem), for suitable ranges of the energy.

Beyond this, when we continue going down in the left part of figure 5 we see some additional maxima close to the last invariant curve for values of ρ slightly less than 0.25. As locally near the elliptic point ρ decreases, we must have a minimum also. For some intermediate value of c, between this situation and the bottom of the left figure, both extrema coincide at a point where the first and the second derivatives of ρ are zero. Note that here we are talking as if the map were "integrable" in this domain, that is, completely foliated by invariant curves. This is not true, but it is not too far from the real behavior. On the right part of figure 5 all the evolutions seem to be monotonically decreasing.

Going back to the top of the left part on figure 5, it is worth to mention that for trace $= -2$ there is also a last invariant curve. In fact a curve of this type subsists for values of the trace less than -2, despite the fixed point is hyperbolic and two 2–periodic elliptic satellites are born by period doubling. The last invariant curve encloses the two satellites. This is easy to understand. The last invariant curve do not cares too much if the fixed point inside has bifurcated to something unstable. This is not his problem!

Figure 6 shows a detailed illustration of the lack of monotonicity of ρ as a function of y_0. The *twist* character has been lost. However there can still exists *non–graph invariant* *curves*, as shown on the right part of the figure. This is a generic situation (cf. [12]). To make these curves “visible” it is convenient to look for values of c such that the value of ρ at the maximum is close to a rational number, m/n, with n small. In the present case the rational 3/10 has been used, but any rational between, roughly, 5/22 and 1/3, not too close to 1/4 or 1/3 produces similar pictures.

We can ask ourselves about the behavior when the “last” invariant curve turns out to be located at a place such that the corresponding rotation number is close to an extremum. In the present situation, that is, studying the invariant island around an elliptic fixed (or periodic) point, this has not too dramatic consequences. In fact SPM is a map on the cylinder, but our study of the island is, locally, in $\mathbb{R}^2$. However, think about the following: Imagine you have a map on $\mathbb{S} \times \mathbb{R}$ or in $\mathbb{T}^2$ with invariant curves which separate two large chaotic regions. The curves prevent from diffusion from one region to the other. When moving parameters the invariant curves can be shifted to a resonant domain and disappear. This resonant domain is much larger if the rotation number is close to an extremum, that is, when the twist character is lost. It can happen that diffusion appears, but later on, moving again the parameters, there is place once more for a separating invariant curve slightly outside the resonant domain. Assume our map depends on two parameters. It can happen that there are “holes” in the parameter space for which no invariant curve prevents from diffusion, completely surrounded by values of the parameters for which invariant curves exist. This is illustrated in Appendix C in [1], for a map which has a strong non–twist character.

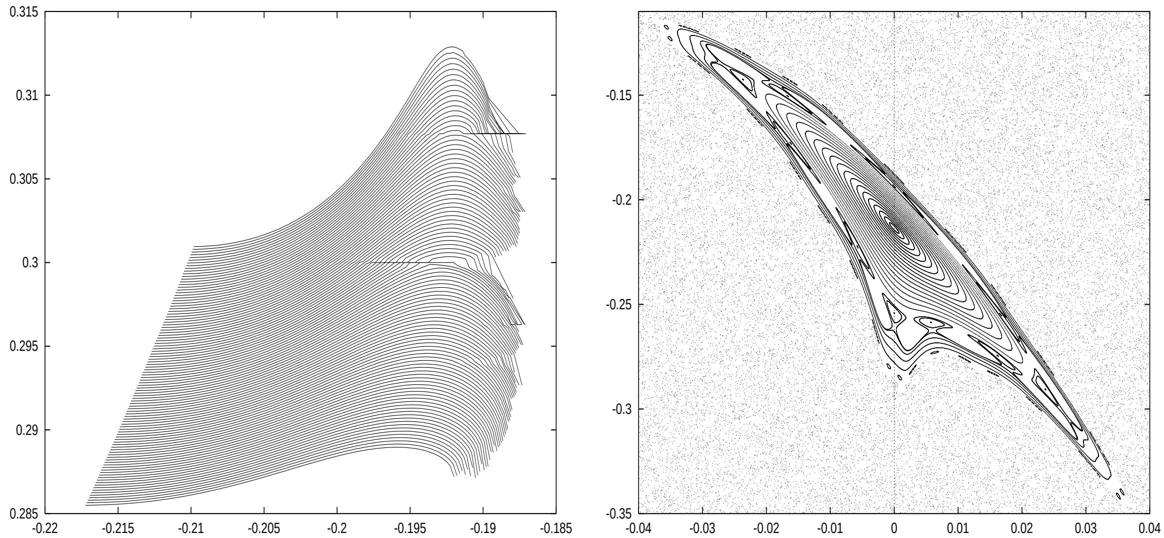

Figure 6: Left: Magnification of a non monotone part of Fig. 5. Also a larger number of values of c has been used. The 3 to 10 resonance is clearly seen. Right: A stable domain showing the non–graph invariant curves associated to a maximum of the rotation number close to 3/10. The value $c = 0.403260832$ has been used.

Concerning the rotation number of the last invariant curve, renormalization ideas (see, e.g., [5] and [8]) give evidence that it must be a “noble” number, that is, all the quotients of the continued fraction expansion are equal to 1 from some point on. In the present example systematic checks have been done on the structure of the phase space around the last invariant curve. This can be done by successive magnifications of smaller and smaller areas. In some sense the mechanism is always the same, in good agreement with what is suggested by renormalization. However, usual schemes for renormalization are addressed at the destruction of an invariant curve with a fixed rotation number when the perturbation parameter is changed. Here the problem is different, because one is interested on the changes of the last curve. Anyway, a study near a given resonance should also provide information about the destruction of nearby curves by the effect of higher order satellite resonances.

A refinement of the rotation number of the last invariant curve has not been considered. Anyway, a rough exploration has been done of the full list of rotation numbers obtained. As it is well known, for a random set of numbers in $[0,1)$, the probability of finding k as one of the quotients of the continued fraction expansion is given by

$$\frac{1}{\ln 2}\ln\left(\frac{(k+1)^2}{k(k+2)}\right).$$

We have computed these quotients for all the rotation numbers obtained, by skipping the first quotient (this would be biased because all the numbers considered are less than $1/2$). The results show a little excess (about $6-8\%$) of 1's and 2's in the data. But further refinement would be necessary for definite conclusions.

Finally we want to comment on a different aspect: the rate of escape of points not being confined for all time on a (perhaps large) vicinity of the fixed point. This is a topic which attracts a strong interest, because of the practical implications. We refer to [9] and references therein for some results, specially concerning the case of the Hénon area preserving map. It is interesting to be able to predict, from a finite time simulation, which is the rate of escape of the points initially located on a given box of the phase space. And, specially, the measure of the points confined for all time. But we note that the case of area preserving maps (or, equivalently, of 2 degrees of freedom Hamiltonians) has very special features. Indeed, the confined points need not to be on invariant tori. They can be in a chaotic zone confined between tori. This is quite different from the case of higher number of degrees of freedom, where maximal dimension tori do not confine. In that case one should expect rates related to the known bound on rates of diffusion, that is, if r_n denotes the amount of points which do not escape after iterate number n, one should have

$$r_n = L + \frac{A}{(\log n)^\beta},$$

where L (eventually zero) are the points which subsist for all time and A, β are positive quantities. This requires a large amount of initial points and a large amount of iterates, to allow for local irregularities. Furthermore some transient (e.g., the first 1000 iterates) has to be skipped, the behavior being too irregular. Then one should be able to find formulas like the previous one. See [11] for an example with three and one half degrees of freedom, where these expectations are confirmed, and where a sketch of the analytical ideas is presented.

4 Discussion

A reliable method has been proposed and largely tested to locate the last invariant curve around an elliptic fixed point. Several points can be mentioned when we look at the evolution of the last invariant curve in a one–parameter family of maps.

- The rotation number of the last invariant curve can never take a rational value. So the graph of ρ_{last} as a function of the parameter must jump over all rationals, leading (at least) to a countable number of discontinuities.

- The same thing is true for the area enclosed by the last invariant curve, that is, the area of the maximal invariant island around the fixed point. Both graphs have a strong fractal character with several similarity properties.

- The mechanism leading to the change of the area is just the "absorption" or "expulsion" of a chain of islands. When the period of the islands is high it is quite reasonable that they are extremely narrow. So, both the jump in rotation number and in area are small, specially last one.

- Typically the invariant curves which come close to a periodic hyperbolic orbit can approach more the periodic orbit if that one is outside the curve than if it is inside. Hence, when there is a jump from, say, $m/n-\delta_1$ to $m/n+\delta_2$ in the rotation number of the last invariant curve, there is a lack of symmetry between δ_1 and δ_2. If the rotation number is decreasing when the distance to the elliptic point increases (as it happens for the separatrix map in most of the cases) then one has $\delta_1 > \delta_2$.

- A study near a given resonance using renormalization should provide useful information about the destruction of nearby curves by the effect of higher order satellite resonances.

- Several other points, concerning the relation between the last invariant curve and invariant manifolds of hyperbolic objects, or rates of escape from some bounded domain, are also presented.

Acknowledgments

The authors are indebted to À. Jorba and J. Meiss for helpful comments on a previous version of this paper. The first author has been partially supported by the EC grant ERBCHRXCT940460, DGICYT grant PB 94–0215 (Spain) and CIRIT grant 1998SGR–42 (Catalonia), who also supported visits of the second author to the University of Barcelona. Both authors are indebted to INTAS grants 93–339ext and 97-0771.

References

[1] Broer, H. W., Simó, C., Tatjer, J. C.: Towards global models near homoclinic tangencies of dissipative diffeomorphisms. *Nonlinearity*, **11** (1998), 667–770.

[2] Dullin, H. R., Meiss, J. D., Sterling, D.: Generic Twistless Bifurcations. Preprint, 1999. Available at `chao-dyn/99010225`.

[3] Filonenko N. N., Sagdeev R. Z., Zaslavsky G. M.: Destruction of magnetic surfaces by magnetic field irregularities. *Nuclear Fusion*, **7** (1967), 253–266.

[4] Gómez, G., Llibre, J., Martínez, R., Simó, C.: *Study on orbits near the triangular libration point in the perturbed restricted three–body problem.* ESA Technical Report, 1987, 270 pp.

[5] Greene, J. M., MacKay, R. S., Stark, J.: Boundary circles for area preserving maps. *Physica D*, **21** (1986), 267–295.

[6] Laskar, J., Froeschlé, C., Celletti, A.: The measure of chaos by the numerical analysis of the fundamental frequencies. Application to the standard mapping. *Physica D*, **56** (1992), 253–269.

[7] Laskar, J.: Introduction to frequency map analysis. In *Hamiltonian Systems with Three or More Degrees of Freedom*, C. Simó (Ed.), NATO ASI, Mathematical Physics Series, Vol. 533, 134–150, Kluwer, Dordrecht, 1999.

[8] MacKay, R. S.: *Renormalization in Area–preserving Maps*, World Scientific Publ., Singapore, 1993.

[9] Meiss, J. D.: Average Exit Time for Volume Preserving Maps. *Chaos*, **7** (1997), 139–147.

[10] Simó, C.: Stability of degenerate fixed points of analytic area preserving mappings. *Astérisque*, **98–99** (1982), 184–194.

[11] Simó, C., Gómez, G., Jorba, À., Masdemont, J.: The Bicircular Model near the Triangular Libration Points if the RTBP. In *From Newton to Chaos: Modern techniques for Understanding and Coping with Chaos in N–Body Dynamical Systems*, Editor A.E.Roy, Plenum Press 1995, 343–370.

[12] Simó, C.: Invariant Curves of Perturbations of Non Twist Integrable Area Preserving Maps. *Regular and Chaotic Dynamics*, **3** (1998), 180–195.

[13] Simó, C., Stuchi, T.: Center Stable/Unstable Manifolds and the destruction of KAM tori in the planar Hill problem. Preprint, 1998. Available at `http://www.maia.ub.es/dsg`.

[14] Simó, C., Treschev, D.: Stability islands in the vicinity of separatrices of near–integrable symplectic maps. Preprint, 1997.

[15] Treschev, D., Zubelevich, O.: Invariant Tori in Hamiltonian Systems with Two Degrees of Freedom in a Neighborhood of a Resonance. *Regular and Chaotic Dynamics*, **3** (1998), 73–81.

[16] Zaslavsky G. M. and Filonenko N. N.: Stochastic instability of trapped particles and the conditions of applicability of the quasilinear approximation, *Zh. Eksp. Teor. Fiz.*, **54** (1968), 1590–1602, (in Russian).